ORIGINAL PAPER

A NOVEL HIGH-SPECIFIC-ENERGY PERMANENT MAGNET SYNCHRONOUS MOTOR WITH TWO STATORS, A SINGLE ROTOR, AND AN AXIAL AIR GAP

MIHAIL FLORIN STAN[1*], IULIAN BANCUTA[1], ALEXANDRU MIHALCIOIU[2], ALEXANDRU NICULESCU[3]

Manuscript received: 11.06.2025; Accepted paper: 27.11.2025; Published online: 30.12.2025.

Abstract. *Brushless permanent magnet motors with axial air gaps are attractive solutions for electric vehicles because of their high-power density, improved efficiency, and simple mechanical design. Recent designs, which may feature multiple stators or rotors, can be categorized based on their mechanical structure into two groups: one with an external rotor and the other with an internal rotor and two stators. The synchronous machine described in this paper introduces original elements by the authors. Having a double stator and axial air gap, it consists of a disk rotor with permanent magnets placed between two stators, between the rotor and stator there being plane air gaps.*

Keywords: *Double stators; unique rotor; high-specific-energy permanent magnet; axial airgaps; electromagnetic analysis; finite element analysis.*

1. CONSTRUCTIVE SOLUTIONS OF SYNCHRONOUS MOTORS WITH AXIAL AIR GAPS USED OR KNOWN FROM THE LITERATURE

The construction of brushless servo motors with disc rotor and axial flux has been adopted to reduce the axial size of the electric machine, for example, for the realisation of industrial robots, machine tools, and electric vehicles. The classic construction of a disc rotor servo motor consists of a disc rotor (on which the axially magnetised permanent magnets are placed) and two wound stator shields, powered by a voltage inverter [1, 2].

For certain advantages, such as a relatively low moment of inertia and a low specific mass, due to the improvement of conditions for heat transfer to the outside, brushless motors with disc rotors are constructed, in which the direction of the magnetic field in the motor is parallel to the shaft. To reduce the moment of inertia and obtain a flat geometry, the servo motor construction with disc rotor and axial intermer can be used [3].

González-Parada et al. [4] demonstrate that some new configurations of electric motors, such as axial flux motors (AFM), can be coupled directly without the use of gearboxes, given their characteristics of high torque at low speeds. The authors introduce an innovative design of a multipolar axial flux motor (MAFM). General criteria for design and construction are presented, taking into account the geometry of axial flux and permanent magnets.

[1] Valahia University of Targoviste, Faculty of Electrical Engineering, Electronics and Information Technology, Department of Automatics, Informatics and Electrical Engineering, 130004 Targoviste, Romania.
E-mail: iulian.bancuta@valahia.ro.
[2] SC Automobile Dacia SA, BodyShop Department, Pitesti, Romania.
E-mail: ion-alexandru.mihalcioiu@renault.com.
[3] Special Telecommunicatios Service, Targoviste, Romania. E-mail: alexandru.niculescu@stsnet.ro.
[*] *Corresponding author: florin.stan@valahia.ro.*

https://doi.org/10.46939/J.Sci.Arts-25.4-c04

Metin et al. [5] suggest that axial flux permanent magnet (PM) machines are being developed for numerous applications due to their attractive characteristics. There is extensive literature on designing a variety of types of axial flux PMs machines. In the work we are referring to, an overview of the different PM machines with axial flow, with and without notches, is given. The machine structures, advantages, and features of the axial flux PM machine (AFM) are clarified. Some new and interesting structures of axial flux machines are also approached from various perspectives.

From the specialised literature in the field, it mentions the paper [6], in which Zhuo Hao et al. inform us that axial flux permanent magnet (AFPM) motors are an important type of motor characterised by a compact structure, high power density, and high torque density. The paper analyses and describes the progress of AFPM engines, focusing on their key technologies, including topological structures, design and optimisation methods, and control techniques. Based on these analyses, the main conclusions of the analysis are the following: YASA-type motors (without yoke and with segmented armature) have a great potential for development; multi-objective optimisation design theories can be integrated and applied for design optimisation, and optimal control and sensorless control have an important value in improving system reliability and reducing costs.

Zhao et al. [7] revealed that axial flux permanent magnet synchronous motors (AFPMSM) have been widely used in wind power generation, electric vehicles, aircraft, and other renewable energy applications due to their high-power density, operational efficiency, and integrability. In order to facilitate comprehensive research on AFPMSM, this article analyses developments in research on the design and optimisation of AFPMSM control, introducing and classifying the basic topologies of AFPMSMs and subsequently summarising the key points of optimising the design of core and coreless AFPMSMs.

Nyitrai et al. [8] believe that axial flux permanent magnet synchronous motors (AFPMSM) can be an attractive choice in the case of high torque density requirements or when the drive medium (packing) is geometrically limited to a disc-shaped motor. However, compared to radial flux motors, the modelling possibilities of axial flux machines are less well-documented. In this study, various electromagnetic modelling approaches were compared through an example of an AFPMSM design.

Singh et al. [9] revealed, in their study, a diagram of synchronous machines with permanent magnets (PM). The Axial Flux PM (AFPM) machine is explained in terms of its structure, areas of interest, and features. Some interesting innovative topologies of hub motion machines are also discussed from a variety of perspectives.

In another research, the design process of a TORUS permanent magnet motor (AFPM) with axial flux and double grooves, suitable for direct drive of electric vehicles (EVs), was presented [10]. He used the dimensioning equation and finite element analysis (FEA). The AFPM motor is a high-torque density motor that is easily mounted and compactly fits on the wheel of a vehicle, fitting perfectly on the wheel rim. A preliminary design is a dual-flow AFPM motor with six rotor poles for high torque density and stable rotation. In determining the design requirements, a simple vehicle dynamics model that evaluates the vehicle's performance during a typical cruise trip was considered.

In the following, some configurations of synchronous motors with permanent magnets and axial interpoles from the literature are presented in Figs 1 and 2. The stators of these types of motors can be made with or without slots, in which case the winding is executed on a template, with a conductor insulated with self-stiffening enamel, impregnated or embedded in a casting table, and then glued on the smooth stator yoke.

The stator technology is the same as that of asynchronous disc rotor servo motors. The rotor is made by gluing permanent magnets into the recesses that are cut into a disc of glasstextolite, duralumin, or even titanium for heavy-duty applications. Also, in the case of

more difficult applications, the bonding of permanent magnets is replaced by mechanical reinforcement.

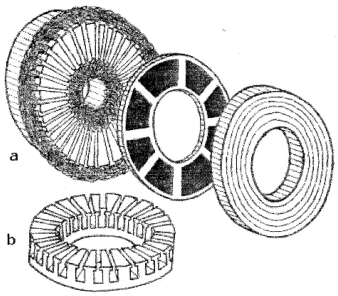

Figure 1. Synchronous servomotor with disc rotor. a) unfolded view; b) stator with slots.

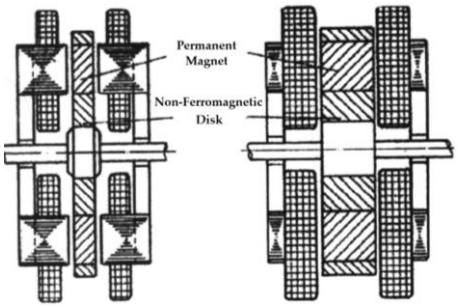

Figure 2. Synchronous servo motor with permanent magnets and a non-ferromagnetic disc.

Synchronous motors with permanent disc rotor magnets are also produced in Romania (Fig. 3), mentioning the SPRD (with slots) and SFCD (without slots) series, with n_N = 3000 rpm and torques up to 4.7 Nm, as well as the SX 14, of 14 Nm, made at ICPE Bucharest.

SmCo magnets and, more recently, NdFeB magnets are used in these motors.

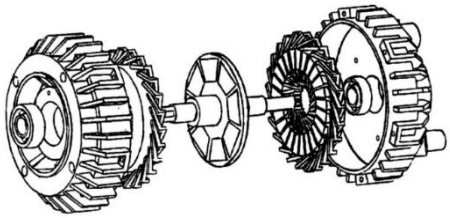

Figure 3. Synchronous motors with permanent disc rotor magnets were produced in Romania.

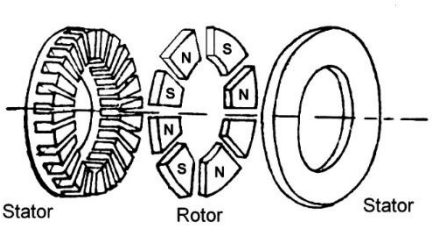

Figure 4. Structure of Synchronous Motor Magnetic Circuit with PMs and Disc Rotor

In Fig. 4, the structure of the magnetic circuit of such a motor is shown. Permanent ferrite or rare-earth magnets are used in the construction of these motors, which lend themselves to a low magnet height and result in a reduced rotor disc thickness.

AlNiCo magnets are unsuitable for this type of motor, due to the low value of the intensity of the coercive magnetic field, which would lead to a high value of the height of the magnet, therefore to a high value of the height of the magnet, therefore to a high value of the thickness of the disc rotor, which would make the main advantages of this type of motor be lost. From a technological point of view, the construction of these engines is different from those with a cylindrical rotor. The stator is made by variable pitch stamping and rolling a siliceous sheet metal strip, and the rotor is obtained by embedding permanent magnets in cast aluminium or other non-magnetic materials.

2. PERMANENT MAGNET SYNCHRONOUS MOTORS WITH TWO STATORS AND A SINGLE ROTOR OR WITH TWO ROTORS AND A SINGLE STATOR WITH AXIAL AIR GAP

2.1. CONSTRUCTIVE VARIANTS FROM THE LITERATURE

AC motors with double stators or rotors and permanent magnets are known in the literature, but their construction is quite complicated, and they are generally made for use in the field of electric vehicles. Double-stator or rotor AC motors, equipped with permanent

magnets, are a specific category of electric motors that utilise these characteristics to enhance performance, efficiency, or power density. These motors can have various configurations, each with its own advantages and disadvantages. Double stator motors typically have a common rotor surrounded by two stators, each with its own windings. This configuration can increase motor torque or allow individual speed control of each stator. In the case of permanent magnet motors, these can be integrated into either the stator or the rotor, thus influencing the operating characteristics. Double rotor motors generally have two independently rotating rotors surrounded by a single stator. This configuration can provide flexibility in speed and torque control, allowing, for example, hybrid operation (series-parallel) or energy recovery. Permanent magnets can be used to improve efficiency and reduce current losses.

Jikai Si et al. in their paper [11] consider that axial flux permanent magnet (AFPM) machines are gaining popularity in low-speed and high-torque applications due to their high torque density, high efficiency, and compact structure. A double-rotor AFPM machine (DRSAFPM) equipped with equidirectional toroidal winding (EDTW) and compared to the one equipped with conventional single-layer and two-layer concentrated windings (SL and DLCW) is proposed. First, the differences between the DRSAFPM machine with EDTW and the conventional concentrated winding machine in terms of coil configuration, electromotive force (EMF), and magnetomotor winding force (MMF) are revealed.

One of the main challenges in EV design [12] is determining the performance of the traction system, as motor power has a direct impact on the size of the battery and the motor itself. Therefore, high power density, efficiency, and torque are essential for the vehicle's range and performance. The study presented in this paper by Augusto Silva and Ricardo Caetano introduces the development of a two-rotor-disc axial synchronous motor designed for the Society of Automotive Engineers (SAE) Formula for light vehicles. It addresses key motor design parameters such as current, terminal voltage, winding configuration, and reactances. The objective was to meet the requirements for the specific dynamics of the vehicle, for example, a wide range of revs, high torque, and dynamic performance. These parameters were validated using finite element simulations, which were then compared to a three-phase induction motor in specialized simulation software.

In [13], Seo-Hee Yang et al. proposed a dual rotor axial flux permanent magnet (DRAFPM) motor to enhance the performance of robotic joints. The DRAFPM motors offer the advantage of reducing iron loss and minimizing volume because they can eliminate the stator yoke. When designing a motor with the same volume, it can be designed to increase the height of the fixed bar by the thickness of the fixed bar yoke and to increase the number of turns. In the case of existing axial flux permanent magnet (AFPM) motors, the shape of the three-dimensional structure is limited by the radial lamination of the stator.

Fariba Farrokh et al. [14] select, design, and analyse three dual stator axial flux switching permanent magnet (DS-AFFSPM) topologies to determine the most efficient structural application for electric vehicles (EVs) based on torque density, power density, and efficiency. Consequently, the topologies entered are thoroughly compared under the same conditions. The results show that the high-power density, high torque density, and high efficiency of the single-tooth internal rotor DS-AFFSPM topology make it a suitable candidate for EV applications because it has the lowest torque ripple.

To meet the various operating conditions of electric vehicles, such as starting, braking, climbing hills at high speed, high-speed cruising, and frequent acceleration and deceleration, Weiliang Wu et al. carry out in [15] the design of a single-magnetic field and dual-stator modulated permanent magnet synchronous motor (DS-FMPM), which uses the inner and outer electrical ports of the double stator to realize cooperative excitation and multimode

operation of the motor and focuses on improving torque density, power density and motor efficiency.

Some constructive configurations found in the literature of the analysed field of synchronous motors with PM and axial air gap are presented in Fig. 5.

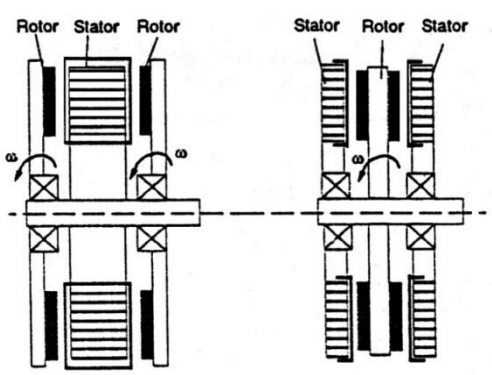

a) **b)**

Figure 5. Permanent magnet motors with axial interference - a) Version with external rotor; b) Version with internal rotor.

The variant in Fig. 5b, with the inner rotor, has two stators, provided with notches on the side facing the rotor, and a rotor equipped with permanent magnets arranged axially, which rotates between the two stators.

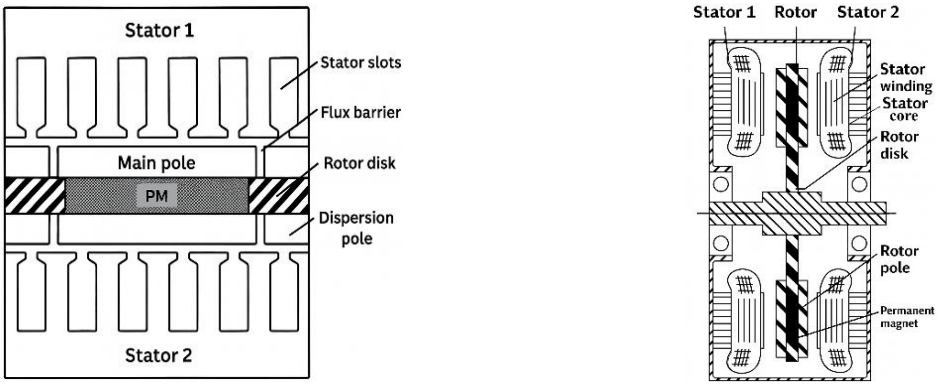

a) **b)**

Figure 6. Motor with a double stator and disc rotor. a) and b) Constructive variants.

Figures 6a and 6b show a dual-stator and disc rotor motor variant. Each of the 2 stators has a ring-shaped core with open notches on the side facing the rotor. The stator polyphase windings are placed in the stator notches.

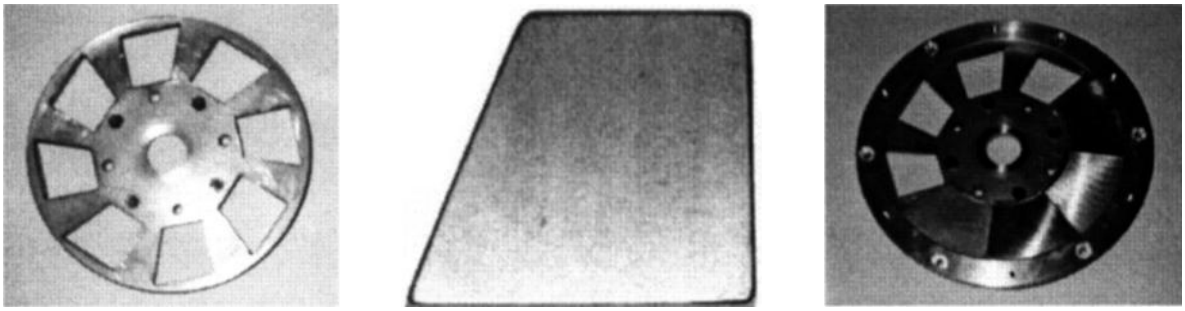

a) **b)** **c)**

Figure 7. Motor with a double stator and disc rotor. a) Rotor made of aluminum alloy in the shape of a disc; b) Permanent magnet; c) PMs fixed with two steel rings.

The two stators are symmetrically fixed in the mechanical structure of the motor, and the rotor is made of an aluminum alloy, having the shape of a disc (Fig. 7a), and is fixed directly to the shaft. The permanent magnets are placed on the rotor (Fig. 7b), being placed in the cutouts made in the rotor disc. Both the rotor disc and the permanent magnets have the same thickness.

On the two sides of the rotor disc, the permanent magnets are fixed by means of two steel rings (Fig. 7c). The two solid steel rings give the rotor a mechanically robust construction and have the role of keeping the magnets permanent in the disc rotor cutouts.

One of the most interesting features of motors with an axial air gap is the ability to mount multiple stators or rotors on the same shaft [16,17]. Aceste structuri neconvenţionale au avantajul unei mai bune exploatări a materialelor folosite.

Fig. 8 shows a motor with two stators and a disc rotor with an axial nozzle.

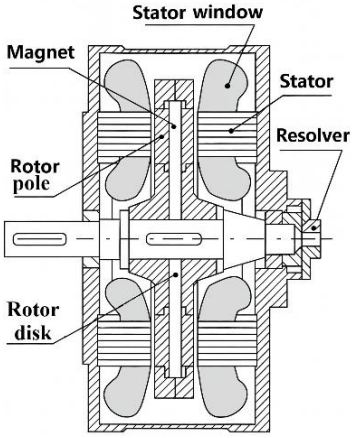

Figure 8. Schematic representation of the two-stator motor and disc rotor with axial indentation.

As can be seen from the previous figure, the motor has a disc rotor that rotates between two stators. Compared to the classic versions of permanent magnet motors, the new structure has the advantage of using a smaller number of magnets.

The stator cores are provided in the part facing the rotor with notches in which the stator windings are placed. The bundle of plates is perpendicular to the magnetic field lines, the notches being positioned radially.

The two stators and the stator windings positioned in the notches are placed symmetrically. In this mode, the impeller must be equipped with magnetic flux closure paths. Engines of this type are, in conclusion, small in size.

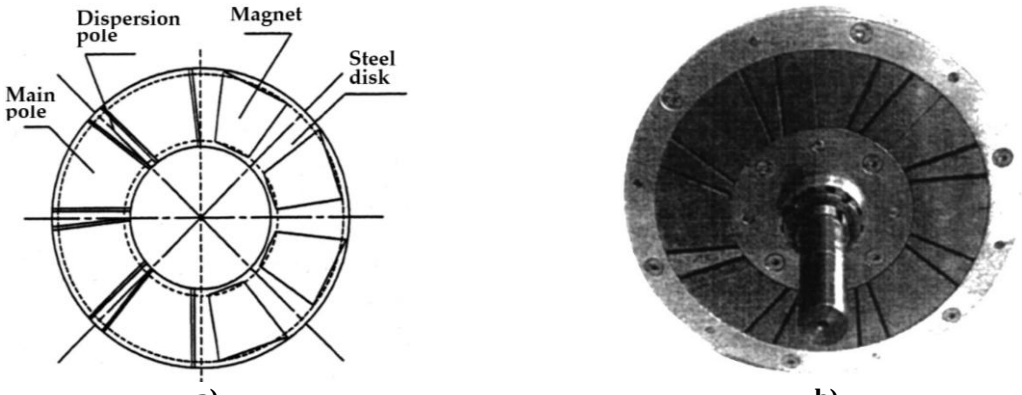

a) **b)**

Figure 9. Motor with two stators and a disc rotor with axial input. a) parts of PMs synchronous motor; b)

PMs fixed with two steel rings.

The two stators are mechanically fixed to the housing, and the stator windings are connected in series. The permanent magnets are located in the rotor disc (Fig. 9a). On the two sides of the rotor disc, the permanent magnets are fixed by means of two steel rings (Fig. 9b).

The two solid steel rings provide the rotor with a mechanically robust construction and serve to keep the permanent magnets in place within the disc rotor cutouts. For each rotor pole, two gaps (flow barriers) are cut into the rotor rings. This creates the main poles and the poles of loosening the flow. The rotor poles make the placement of permanent magnets much simpler, and the mechanical structure is much more robust.

The shape of the magnets and main poles must be chosen in such a way as to maintain a constant ratio between the magnetic and stator poles throughout the radius of the machine. Consequently, the active conductors are subjected to the same magnetic field along their radial length. Moreover, the magnets are not symmetrically arranged for flow barrier escapes. This complex rotor structure is only achievable with the help of soft magnetic powders. In fact, to achieve losses due to low eddy currents, the rotor poles cannot be made of solid steel, and the flow barriers cannot be made of rolled material.

2.2. REDUCTION OF PARASITIC COUPLES BY PLACING NON-SYMMETRICAL (DEVIATION) OF THE POSITION OF THE MAGNETS ON THE ROTOR

In motors with permanent magnets, with the stators provided with notches, parasitic torque occurs due to the interaction between the magnets on the rotor and the iron teeth on the stator – "cogging torque". This torque negatively influences the speed control performance, especially at low speeds, producing vibrations and noise, which are amplified when the torque frequency coincides with a mechanical resonance frequency of the stator or rotor. Several methods of reducing the value of this parasitic couple are known in the literature [18-21].

In classic construction, the impeller has the configuration of Fig. 10, where, for simplicity, the mechanical structure of fixing the magnets is not shown.

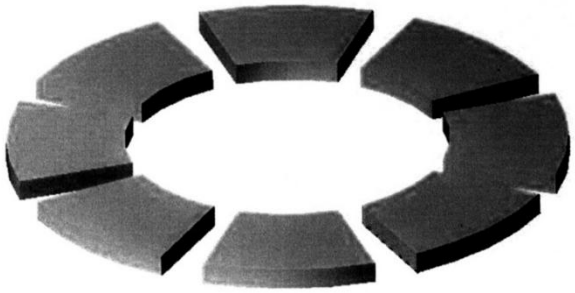

Figure 10. Rotor configuration with axial input, without additional presentation. Mechanical structure for fixing permanent magnets.

It is known that the period of the parasitic torque depends on the smallest common multiple (s.m.m.) between the number of notches and the number of magnetic poles on the rotor.

For example, for a tile with 24 notches and 8 poles, c.m.m.m.c. is 24, so the period of the parasitic torque is equal to 360° / 24 = 15°.

Fig. 11 shows a solution used to reduce this torque. The solution consists of deviating the position of the single-polarity magnets from the reference axes shown, in the direction indicated, at an angle equal to 360° / ($2 \times Z$), where Z is the number of notches.

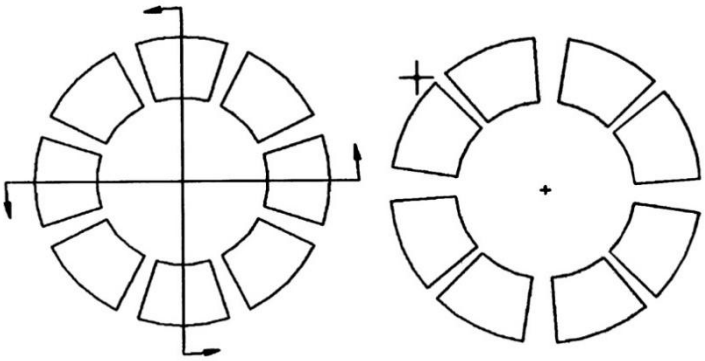

Figure 11. The solution adopted for the reduction of parasitic torque (cogging torque).

Fig. 12 shows the curves of the parasitic torque before and after the displacement of the magnets.

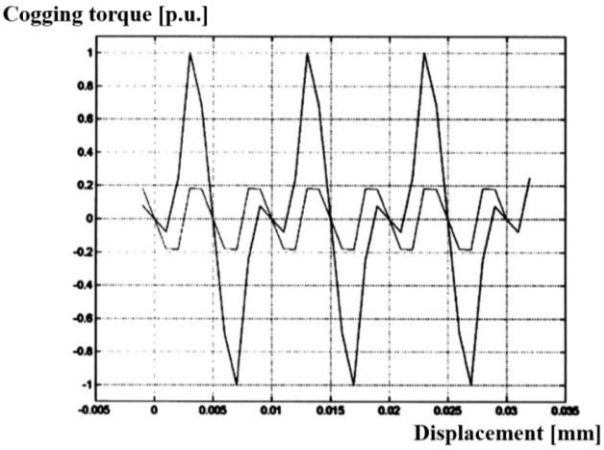

Figure 12. The curves of the parasitic torque before and after the displacement of the magnets.

2.3. CONSTRUCTION OF STATORS FOR AXIAL INPUT MOTORS. VARIANT WITH MAGNETIC CIRCUIT ROULETTE TYPE WITH VERTICALLY MILLED NOTCHES.

The construction of the stator can be done with a stator magnetic circuit obtained by rolling and radial milling of the notches, as shown in Fig. 13.

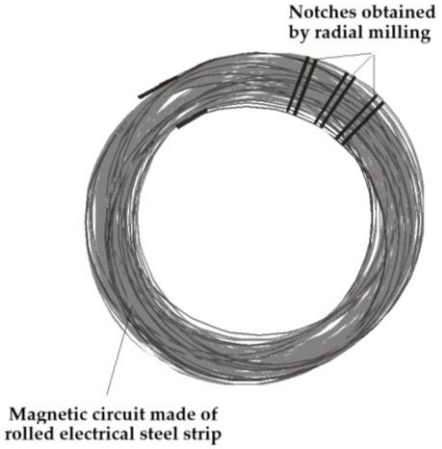

Figure 13. Stator magnetic circuit obtained by rolling and radial notch milling.

The notches are obtained by radial milling through the sheet pack, as shown in Fig. 14.

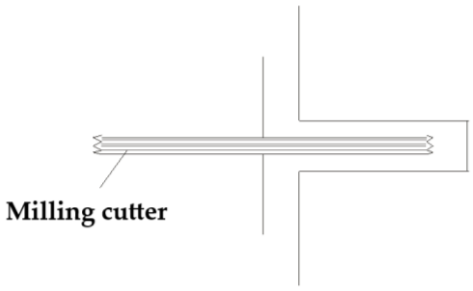

Figure 14. Grooves obtained by radial milling.

The disadvantages of this method are: milling through the sheet metal package is cumbersome due to vibrations; the notches obtained are open; due to the milling process, the sheets will be short-circuited.

3. VARIANT OF PM SYNCHRONOUS MOTOR WITH TWO STATORS, A SINGLE ROTOR, AND AN AXIAL AIR GAP

The synchronous machine with permanent magnets presented below (Fig. 15) is a contribution of original elements by the authors of this research. Having a double stator and axial air gap, it consists of a disc rotor (Fig. 16) placed between two stators; between the rotor and the stators, there are plane interferences.

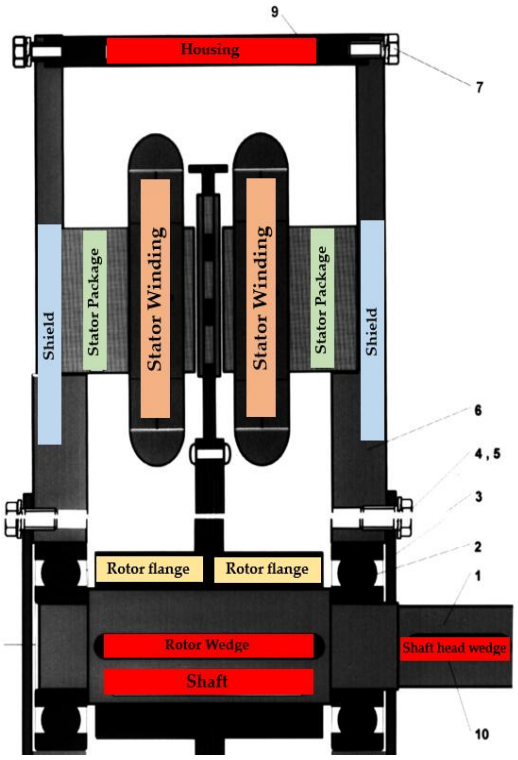

Figure 15. Synchronous machine with permanent magnets with axial interpeller, with polygonal magnetic circuit, composed of stamped sheet segments

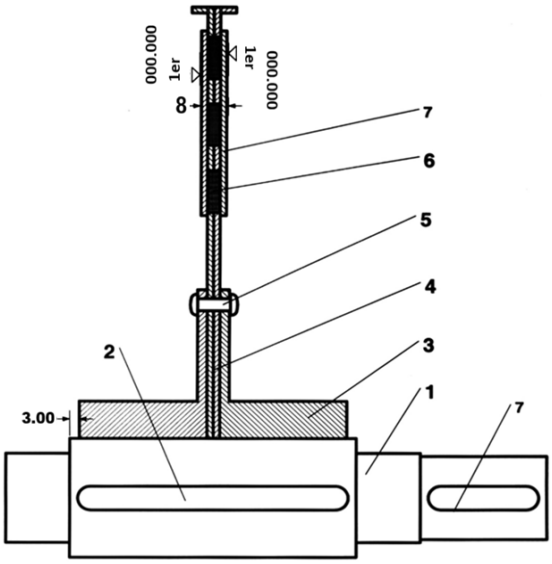

Pos.	Name	Drawing number	Pieces	Material
8	Wedge 8× ×50	CR 006 / 1	1	OL 60
7	Polar piece	CR 004	12	OL 37
6	Permanent magnet	CR 003	90	NdFeB
5	Round head rivet 4×15		6	OL 34
4	Stamped rotor disc	CR 002	2	Aluminum
3	Rotor flange	CR 005	2	OL 37
2	Wedge 8× ×85	CR 006 / 2	1	OL 60
1	Arbor	CR 007	1	OLC 45

Figure 16. The rotor subassembly with permanent magnets of high specific energy (of the NdFeB type), placed on both sides of it.

The disc rotor is made of two thick plates (Fig. 17), stamped from non-magnetic material. To give good mechanical robustness to these sheets, their periphery is bordered.

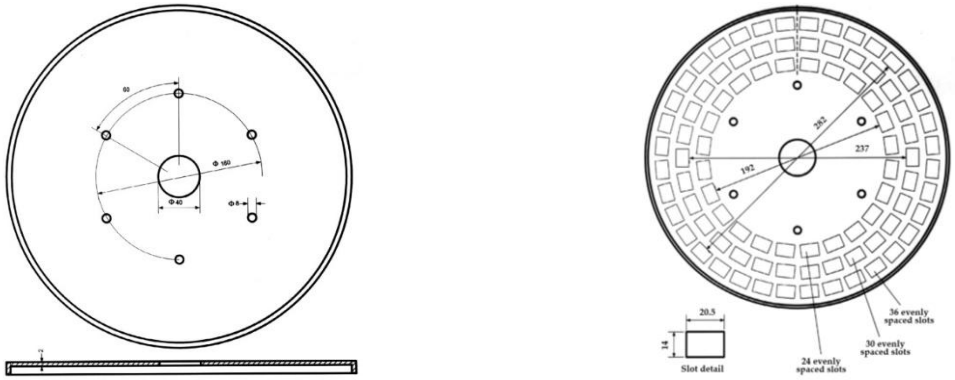

a) **b)**

Figure 17. Rotor disc. a) Cut-out rotor disc; b) Stamped rotor disc.

In some of the stamped slots, permanent magnets are placed (Fig. 18), which generate a magnetic field whose field lines in the two interspheres are parallel and have a direction parallel to the machine's axis.

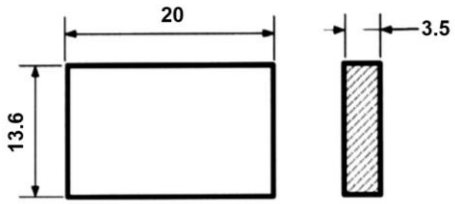

Figure 18. Magnet permanent.

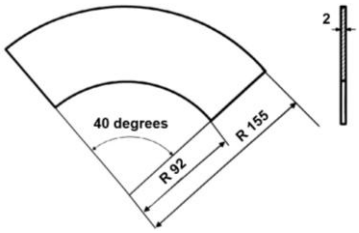

Figure 19. Polar piece.

As a result of the fact that only certain areas of the rotor blades are occupied by permanent magnets, the synchronous machine is built for a certain number of poles, namely $2p = 6$.

To ensure a rotor pole, the permanent magnets in the area of each pole are placed so that they have the same orientation of the magnetic field. Ensuring a magnetic field as uniform as possible at each pole is obtained by means of polar pieces (Fig. 19), which are fixed by glueing, on one side of the rotor and on the other, in the area of each pole.

These pole pieces also have the role of mechanically axially fixing the permanent magnets in the slots in the rotor blades.

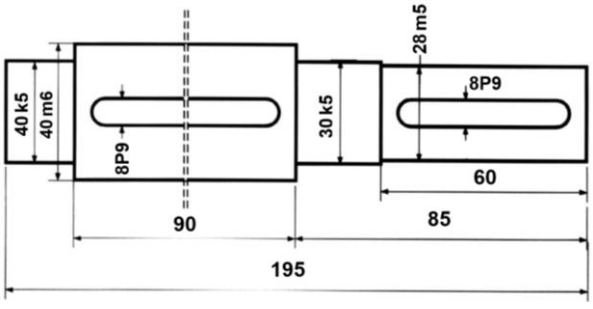

Figure 20. Machine shaft

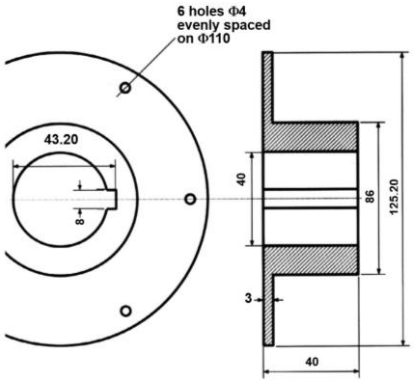

Figure 21. Rotor flange

The rotor plates, bearing the permanent magnets assembled with the pole parts, are mounted on the machine shaft (Fig. 20).

In order to ensure that the rotor plates are placed in a plane perpendicular to the axis of the machine shaft, a rotor flange is fixed on either side of these plates (Fig. 21).

The tangential fixing of the rotor plates and flanges is carried out with the help of a wedge buried in the machine shaft.

On either side of the rotor, there is a stator, composed of bundles of sheets fixed by welding to a shield of the machine. In these bundles of sheets on each shield, which constitute a shield with a magnetic circuit, the stator winding is placed, resulting in the shield subassembly with a winding magnetic circuit. The two shield subassemblies with wound circuit have an identical construction, but they are mounted in relation to the rotor so that the electromotive voltages induced in them are additional.

Difficult to achieve, as has already been shown, are the magnetic circuits of the stators. A toroidal configuration of each magnetic circuit would apparently be useful, but technologically, it is disadvantageous. For this reason, we resorted to a polygonal shape of the magnetic circuit of each stator. A polygon with 12 sides was chosen. Each side of the polygon is made using stamped sheets (Fig. 22) assembled in packages, fixed with rivets (Fig. 23) between an inner frame (Fig. 24) and an outer frame (Fig. 25).

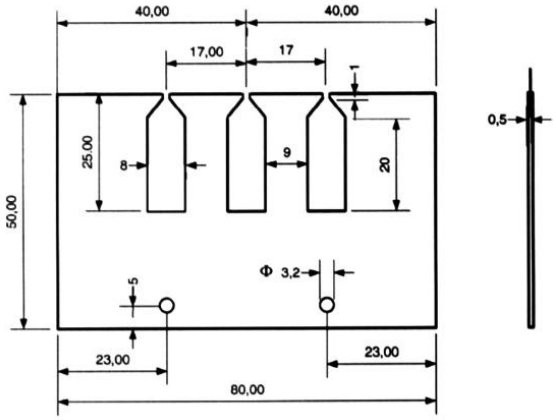

Figure 22. Stator plate.

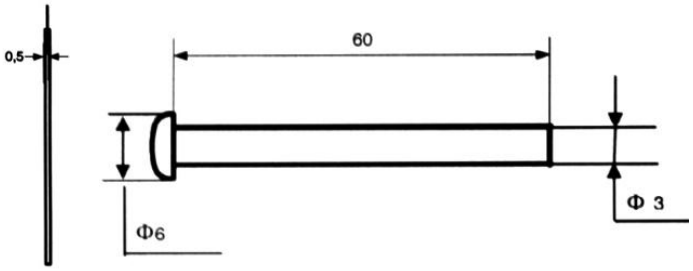

Figure 23. Rivet of stator package.

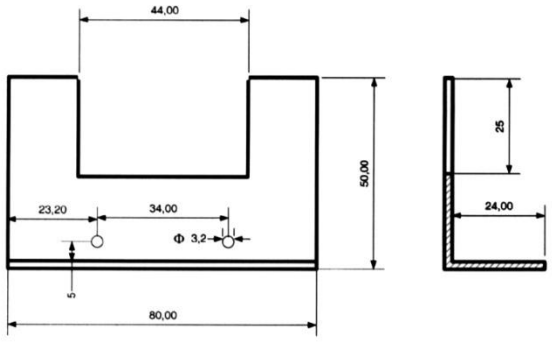

Figure 24. Stator package outer frame.

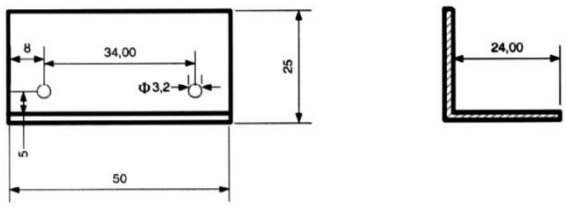

Figure 25. Stator package inner frame.

Taking into account the polygonal shape of the magnetic circuit, the corners of each sheet pack are processed, after which they are fixed by welding on a shield. In order to be able to position the sheet metal bundles in a polygonal configuration, the shields are machined with polygonal edges.

The shields and stators with milled exterior are mounted on the housing (Fig. 26 – a and b) by means of flanges (Fig. 27 - a and b).

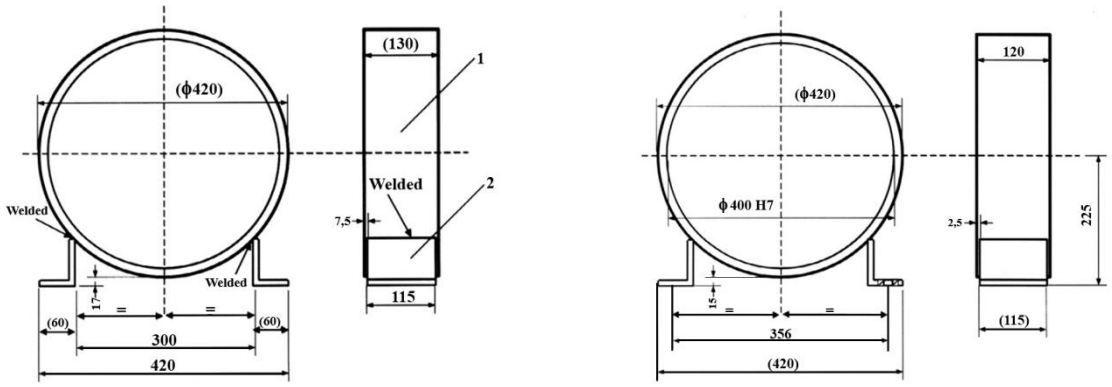

a) **b)**

Figure 26. Machine housing. a) welded housing; b) machined housing

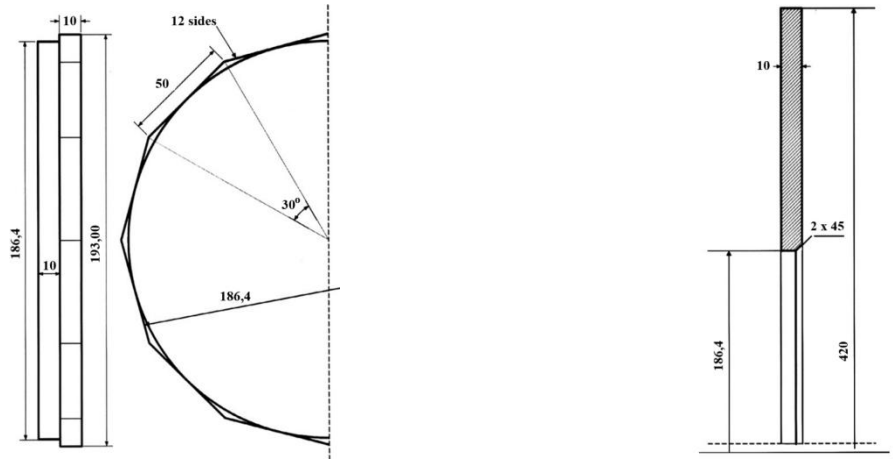

a) **b)**

Fig. 27. Shield and stator flanges. a) stator flange with milled exterior; b) shield flange.

4. EXECUTION AND CERTIFICATION OF THE EXPERIMENTAL PROTOTYPE

4.1. CONCEPTION AND EXECUTION OF THE PROTOTYPE

A series of construction processes used in the realisation of magnetic circuits for the stators of alternating current motors with axial interference is well known.

The most often used and most efficient in terms of reducing iron losses consists in making the magnetic circuit from electrotechnical steel strip, alloyed with silicon, by rolling (roulette type) after which the stator notches are milled vertically, with the help of circular cutters, on special devices with dividing head, which allow obtaining a constant angle between the axes of the notches.

However, this process has several disadvantages, among which can be mentioned: the difficult compaction of the slabs, the mechanical processing by milling the notches in lamellar toroidal packages (leading to an increase in iron losses through the short-circuit bridges that occur during processing, obtaining only open notches) with the known disadvantages for the

electromagnetic parameters of the machine and the more difficult mechanical assembly of the stator subassembly.

Other execution processes are also known, such as making the magnetic circuit out of solid steel, or arranging the windings in the air, on a magnetic support, all of which cannot be compared, in terms of the electromagnetic performance of the machines, with the process described below.

This process of building the stators of alternating current machines removes the disadvantages presented above by the fact that the toroidal magnetic circuit is divided into several sectors, each of which is made of flat plates in which the anchors have been stamped, before wrapping, by the classical processes.

In order to eliminate the parasitic interferences that may occur when assembling the magnetic circuit, after packing each sector, the surfaces that are to come into contact with the neighbouring sectors are polished, all of which are guided on a flange that also constitutes the bearing shield of the machine.

The winding of the stators is similar to that of classic three-phase alternating current machines, the operation being simpler because it is performed on a flat, completely free surface.

The following describes how to create the magnetic circuit for a machine with an axial interlock and six poles, as illustrated in Figures 28-31.

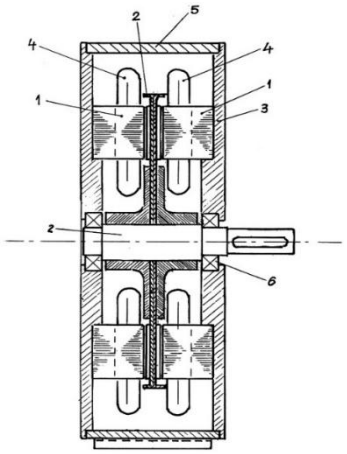

Figure 28. Longitudinal cross-section by axial interlock machine.

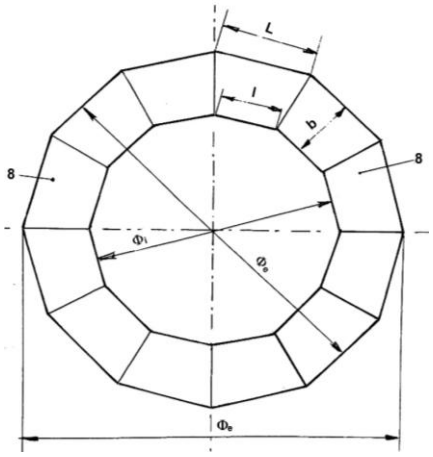

Figure 29. The toroidal magnetic circuit, divided into several sectors, of the stator of the axial input machine.

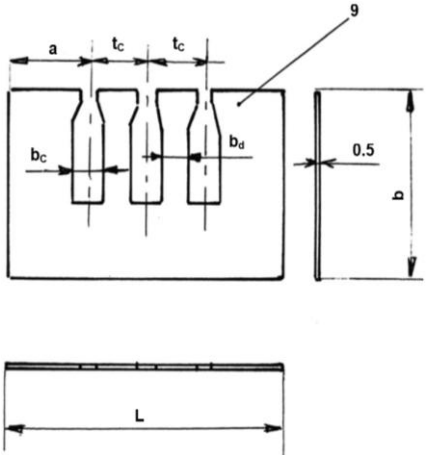

Figure 30. Stamped stator sheet, with notches.

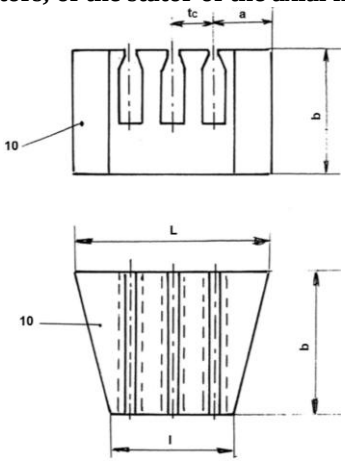

Figure 31. Sector de circuit magnetic stator, assembled and finished.

The magnetic cores (1) of the two symmetrical stators surrounding the permanent magnet disc rotor (2) are fixed on a bearing disc (3). In each magnetic core are arranged the three-phase windings (4). A thin cylindrical housing (5) and bearings (6) ensure that the rotor is centred in the machine assembly. The toroidal magnetic circuit of the stator is divided into twelve sectors (8), consisting of commonly stamped plates (9) assembled into packages (10).

The above construction process for the realization of the magnetic circuit of the stators of the axial interlock machines has the advantage of an easy and precise realization, through a normal stamping operation of the notched sheets, by sectors, followed by an assembly of the sectors and their fixing in the bearing-bearing shield plate, this machining allowing the realization of a compact mechanical subassembly and having superior electromagnetic parameters.

Fig. 32 shows various parts of the motor with two stators and a single rotor with axial interference, made in the prototype laboratory of SC UMEB SA.

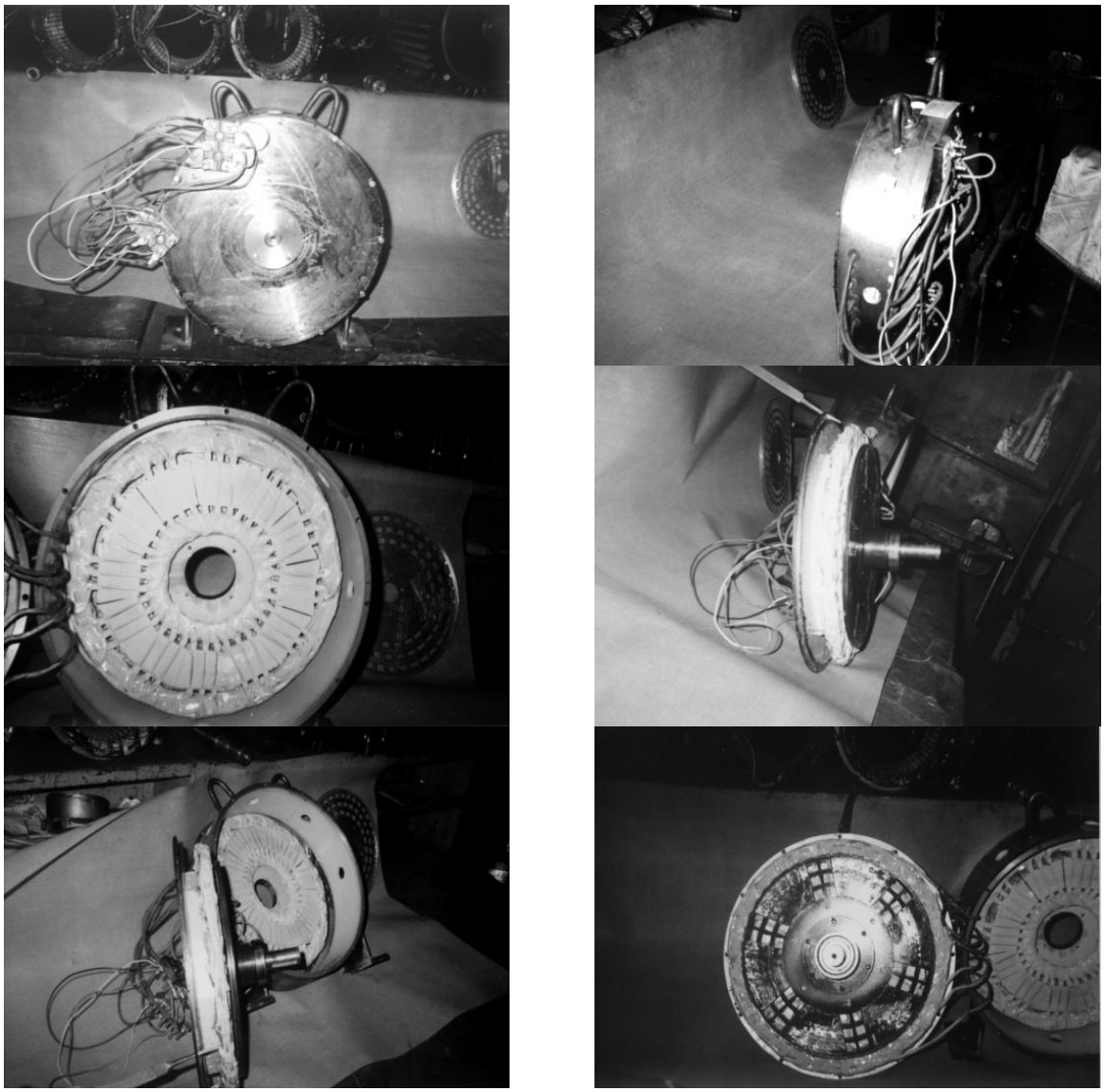

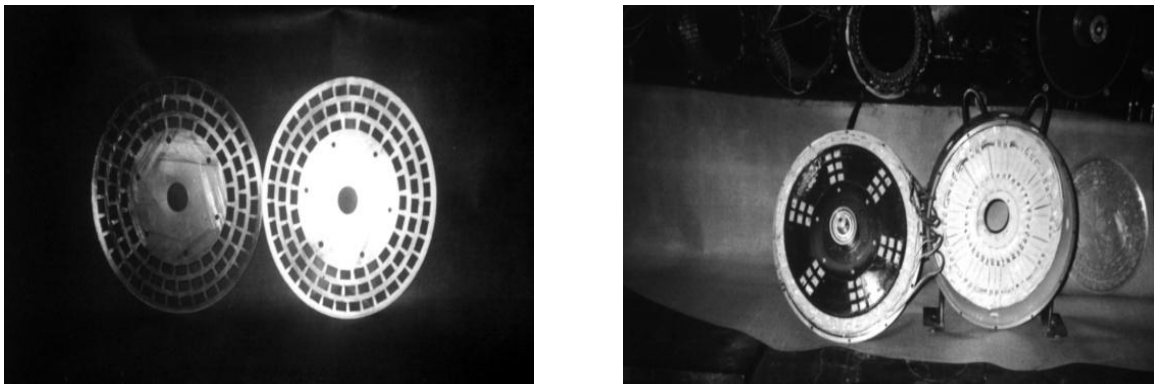

Figure 32. Parts of the prototype have been made.

4.2. SIZING OF PERMANENT MAGNETS FOR THE EXPERIMENTAL PROTOTYPE OF SYNCHRONOUS MOTOR WITH TWO STATORS AND SINGLE ROTOR WITH PERMANENT MAGNETS, WITH AXIAL INTERMER

In the case of the experimental prototype achieved in cooperation with S.C. U.M.E.B. – S.A. (prototype workshop), it was expected that the permanent magnets with rare earths delivered by S.C. I.C.P.E. – S.A., respectively NdFeB, with Br = 1.05 T and Hc = 600 kA/m.

By constructing the rectangle with the base Hc and the height Br, the following values are obtained for the optimal operating point (R):

$$B_m = 0.7 \text{ T}$$
$$H_D = 350 \text{ K/m}$$

Considering approximately, $A_m \cong A_\delta$, we obtain:

$$H_d = \frac{l_\delta \cdot B_m}{l_m \cdot \mu_0}$$

with $l_\delta = 6 \cdot 10^{-3}$ m and $\mu_0 = 4\pi \cdot 10^{-7}$ H/m it follows:

$$l_m = \frac{l_\delta \cdot B_m}{\mu_0 \cdot H_d} = \frac{2 \cdot 10^{-3} \cdot 0,7}{4\pi \cdot 10^{-7} \cdot 350 \cdot 10^3} = \frac{2 \cdot 7}{4\pi \cdot 350} = 0,0095\, m = 9,5\, mm.$$

Normal as well as the expected values for the length of the magnets are confirmed.

5. EXPERIMENTAL RESULTS OBTAINED FOR THE HYBRID PROTOTYPE MADE ACCORDING TO THE SOLUTION PRESENTED ABOVE

a) Trial schedule

The prototype tests were carried out in the test stand of the central laboratory of SC UMEB SA, thus ensuring the guarantee of total impartiality in the assessment of the results and the possibility of rapid interventions within the test program. The program of the tests was as follows:

A. Tests of good execution and identification: *(i)* progressive rotation up to 1000 rpm; *(ii)* marker marking; *(iii)* measurement of insulation resistance; *(iv)* direct current measurement of the electrical resistances of the windings; *(v)* identification of the phase sequence direction for the two stators.
B. Generator tests: *(i)* determination of idle t.e.m. at 1000 rpm for each stator; *(ii)* setting the stators to give maximum t.e.m.; *(iii)* Characteristic U = f (I) for resistive load; *(iv)* characteristic U = f (I) for fully inductive load; *(v)* characteristic U = f (I) for load with $\cos\varphi = 0.8$.

b) Experimental surveys and data processing are presented in Tables 1-7.

Table 1. Measurement of insulation resistance (with the megohmmeter).

Phase-Ground	**Cold measurement**	
	$R_{iz}[M\Omega]$	θ_a[℃]
Ax-Ground	> 50	18°
By-Ground	> 50	
Cz-Ground	> 50	

Table 2. Direct current measurement of the electrical resistances of the windings.

Stator 1 (n_1 = 100)	$C = 150/1{,}5$	αU	0.25	0.253	0.25
		αI	108.40	108.60	108.7
	$\theta_a = 18$ [℃]	R_θ	0.23	0.23	0.23
		Phase	A-X	B-Y	C-Z
Stator 2 (n_1 = 1000)	$C = 150/1.5$	αU	0.25	0.26	0.26
		αI	108.70	108.70	108.70
	$\theta_a = 18$ [℃]	R_θ	0.23	0.23	0.23
		Phase	a-x	b-y	c-z

Table 3. The t.e.m. value induced at idle at n1 = 1000 rpm.

1 – 2: U [V] = 31.50	2 – 3: U [V] = 32.00	3 – 1: U [V] = 32.00

Table 4. External characteristic (under load) U = f (I), for resistive load.

C = 0.5	αU_1	126.60	121.00	117.20	110.80	100.60	96.00	83.30	72.30	55.50	18.00
	αU_2	128.00	122.30	118.30	112.00	101.00	96.60	83.60	72.00	54.30	20.20
	αU_3	126.60	120.00	116.20	109.00	98.90	94.80	83.40	72.40	55.30	19.00
	$U[V]$	63.60	60.55	58.60	55.30	50.08	47.90	41.70	36.10	27.50	9.50
C = 7.5/100 C = 15/100	αI_1	0.00	21.30	31.50	43.90	62.30	68.60	85.50	49.30	58.40	70.50
	αI_2	0.00	22.80	30.80	43.40	61.70	68.50	83.80	48.00	57.00	69.50
	αI_3	0.00	22.50	32.70	45.70	63.30	70.00	85.60	49.00	58.40	70.70
	$I[A]$	0.00	1.660	2.370	3.32	4.68	5.18	6.370	7.32	8.69	10.53

Table 5. External characteristic (under load) U=f(I) for a fully inductive load.

C = 75/150	αU_1	126.70	120.70	117.00	113.30	110.00	106.70	103.60	100.00	93.30	88.50	84.50	83.30
	αU_2	127.80	121.70	118.70	114.70	110.50	108.70	105.70	103.30	97.80	93.00	90.00	89.00
	αU_3	126.70	121.00	117.00	112.70	107.70	107.00	104.30	100.00	92.50	87.00	82.70	82.70
	$U[V]$	63.50	60.60	58.78	56.78	54.70	53.70	52.27	50.55	47.240	44.75	42.870	42.50
C = 2.5/100 C = 5/100	αI_1	0.00	20.00	29.00	40.20	50.00	63.30	71.80	84.30	52.00	60.30	66.70	68.00
	αI_2	0.00	20.50	31.00	45.30	64.3.00	65.80	76.30	91.00	57.70	68.40	77.70	79.70
	αI_3	0.00	19.00	31.70	46.70	64.7.00	67.00	75.30	86.70	52.30	59.80	64.80	66.40
	$I[A]$	0.00	0.49	0.76	1.10	1.408	1.63	1.86	2.18	2.70	3.14	3.48	3.57

Table 6. Load characteristic U. P. S. $\cos\varphi = f(I)$ for loading with a basket $\cos\varphi = 0.8$.

C = 0.5	αU_1			112.30			112.50			104.30
	αU_2			114.00			113.70			104.80
	αU_3			113.30			113.60			104.40
	$U[V]$			56.60			56.63			52.250
C = 0.5	100.00	98.70	92.30	93.90	94.70	89.80	85.30	79.20	78.30	78.40
	100.30	99.40	92.20	94.30	95.00	89.70	84.70	76.80	77.80	77.50
	99.90	98.70	92.20	93.70	94.60	89.70	85.00	78.60	77.80	78.30
	50.30	53.70	46.10	46.90	47.30	44.80	42.50	39.10	38.90	38.40
C = 0.025	αI_1			56.60		56.63		52.50		55.28
	αI_2			54.00		55.00		89.00		67.70
	αI_3			51.20		50.10		95.00		68.60
	$I[A]$			1.26		1.26		2.21		16.22
C=1.25	αW_1			62.20		61.30		90.00		73.00
	αW_2			18.40		17.20		38.70		27.30
	ΣW			80.60		78.50		128.00		100.30
	P			100.70		98.12		161.00		125.30
	$\cos\varphi$			0.81		0.79		0.80		0.80
	S			124.30		123.40		200.00		155.20
C = 0.05	50.03	53.70	68.20	66.00	63.80	73.30	82.70	61.60	62.80	64.30
C = 0.075	52.70	59.60	69.20	67.00	64.80	72.70	81.60	60.00	61.30	62.80
	55.80		74.30	72.30	69.80	79.30	89.20	65.40	65.30	68.30
	2.65	2.81	3.52	3.42	3.30	3.75	4.22	4.67	4.74	4.88
								$\rightarrow C = 3.75$		
C = 2.5	51.00	53.6	62.6	61.6	59.8	63.7	67.3	45.8	46.3	47.5
C = 3.75	21.20	23.5	30.7	29.3	27.3	29	31.2	20.3	21	22
	72.20	77.1	93.3	90.9	87.1	92.7	98.5	66.1	67.3	69.5
	180.50	193	233	227	217	231	246	247	252	260
	0.78	0.79	0.82	0.81	0.8	0.79	0.79	0.78	0.78	0.8
	229.90	241	282	278	271	291	311	316	319	325

Table 7. Load in the $\cos\varphi = 0.8$

C = 0.075	αU_1	74.00	75.00	73.40	70.20	69.00	69.00
	αU_2	70.30	73.00	72.00	68.30	64.00	66.40
	αU_3	72.70	73.70	73.00	69.00	66.70	67.30
	$U[V]$	36.10	36.90	36.40	34.50	33.20	33.70
C = 3.75	αI_1	72.60	71.30	72.50	78.30	80.30	80.70
	αI_2	70.30	68.40	70.00	74.30	76.30	76.30
	αI_3	76.30	74.80	76.30	81.30	83.50	83.70
	Im	5.48	5.360	5.47	5.84	6.00	6.01
	αW_1	49.70	49.00	49.40	50.00	50.00	49.80
	αW_2	25.00	23.50	24.00	25.30	25.70	25.60
	ΣW	74.70	72.50	73.40	75.30	75.70	75.40
	P	280.10	271.80	275.20	282.00	283.87	282.00
	$\cos\varphi$	0.81	0.79	0.79	0.80	0.82	0.80
	S	343.20	343.10	344.80	350.00	345.99	352.00

The external characteristics for different load types and waveforms are shown in Figs 33 and 34. The Fig. 33 shows the terminal voltage U versus load current I for three load types: resistive. inductive. and a mixed load with $\cos\varphi = 0.8$. As the load current increases. the terminal voltage decreases in all cases due to internal voltage drops and armature reaction effects as follows: *(1)* with a **purely resistive load**. the voltage drop is moderate and relatively smooth; *(2)* for $\cos\varphi = 0.8$. the voltage decreases more noticeably. reflecting the combined effect of resistive and reactive components; *(3)* under a **purely inductive load**. the voltage drop is the most pronounced. especially at higher currents. due to the stronger demagnetizing effect of armature reaction and increased reactive voltage drops. Overall, Fig. 33 highlights how inductive loading worsens voltage regulation compared to resistive loading.

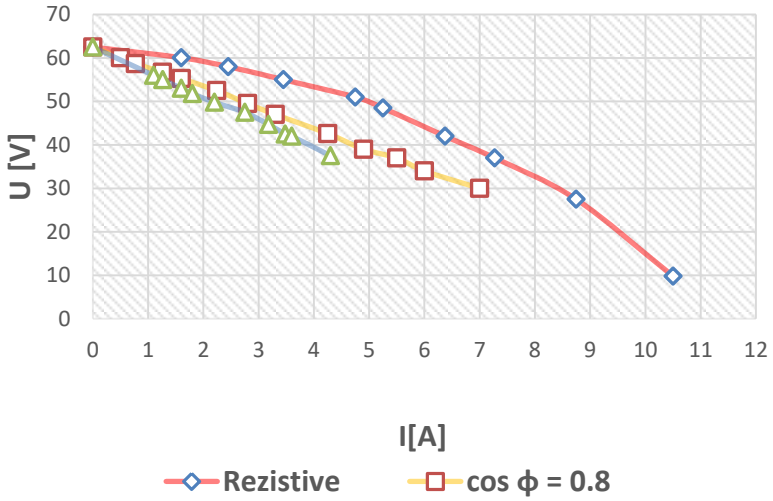

Figure 33. The external characteristics for different load types.

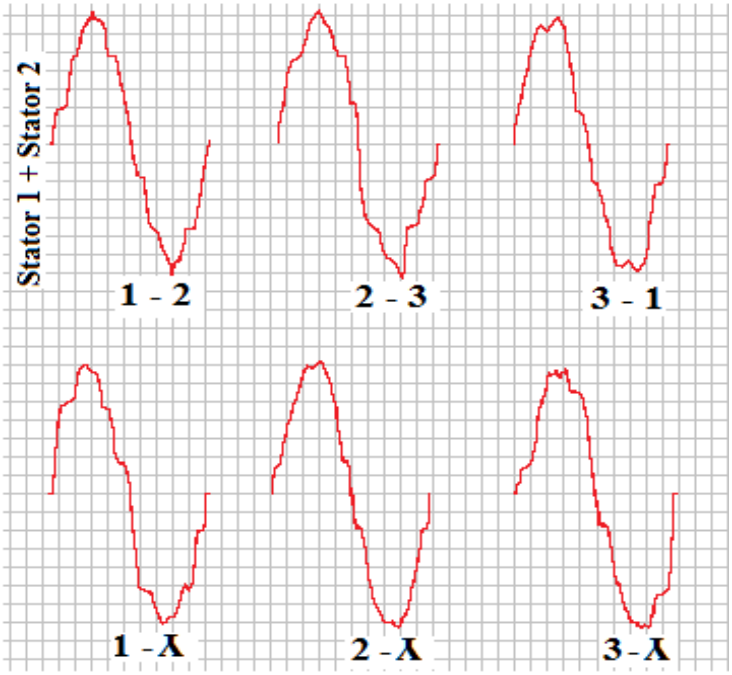

Figure 34. The external characteristics of different waveforms.

The Fig. 34 presents the phase-to-phase and phase-to-neutral voltage waveforms between stator terminals (1–2. 2–3. 3–1. and 1–ʌ. 2–ʌ. 3–ʌ). The waveforms are generally periodic and close to sinusoidal. indicating balanced three-phase operation. Minor distortions and asymmetries can be observed. which are typically caused by magnetic saturation. slotting effects. and non-ideal load conditions. Despite these distortions. the three phases remain well distributed and approximately equal in amplitude. confirming proper machine operation.

6. CONCLUSIONS

For the stator execution of synchronous motors with an axial air gap. the authors proposed a novel constructive solution that proved technically feasible and offers indisputable benefits in terms of the machine's energy parameters and operating characteristics.

The executed prototype was tested as a generator; at the laboratory of SC UMEB SA, there was no frequency converter corresponding to the car's power supply in engine mode.

Each stator has 36 slots. Since the machine is three-phase and has 6 poles. it results in two notches per pole and phase. The stator winding is designed for these sizes. taking into account that the two stators will be serialised for similar phases.

The construction of the machine allows for a variation in the relative position of the two stators. enabling the discovery of a solution with optimal performance.

The realisation of the magnetic circuit of the stators in alternating current machines with axial interference, as proposed by the authors. is a constructive process that utilises insulated flat plates with notches for the placement of windings. This process leads to the reduction of iron losses and eliminates difficult processing. ensuring a simple winding and an easy technological assembly.

This construction process is characterized by the ability to create notches with optimized shapes. either semi-closed or semi-open. when stamping the sheets. This allows for better consolidation of the windings and superior magnetisation characteristics. thereby improving the operating and energy performance of the machine.

REFERENCES

[1] Huang, R., Song, Z., Zhao. H., Liu, C., *IEEE Transactions on Transportation Electrification*, **8**(2), 2118, 2022.
[2] Shao, L., Navaratne, R., Popescu, M., Liu, G., *IEEE Access*, **9**, 158998, 2021.
[3] Nasiri-Gheidari, Z., Lesani, H., *Przegląd Elektrotechniczny*, **88**(2), 300, 2012.
[4] Januar, S. B., Irawan, F., Hadi, W., Sastiko, B. A., *IOP Conf. Series: Materials Science and Engineering*, **1034**, 012053, 2021.
[5] Aydin. M.. Huang. S.. Lipo. T.A.. *Engineering and Technology, Electrical Engineering*, **10**, 1, 2025.
[6] Hao, Z., Ma, Y., Wang, P., Geng Luo, G., Chen, Y., *Machines*, **10**(12), 1178, 2022.
[7] Zhao, J., Liu, X., Shuang Wang, S., Zheng, L., *Chinese Journal of Mechanical Engineering*, **36**, 45, 2023.
[8] Nyitrai, A., Szabó, G., Horváth. S., *Periodica Polytechnica Electrical Engineering and Computer Science*, **66**(2), 205, 2022.
[9] Rajkishor Singh, R., Jadon, J. K. S., Kumar, Y., Bhatnagar, R., *Journal of Emerging Technologies and Innovative Research*, **5**(8), 13, 2018.
[10] Mahmoudi, A., Rahim, N. A., Ping, H. W., *Progress in Electromagnetics Research*, **122**, 467, 2012.
[11] Jikai, S., Tianxiang, Z., Rui, N., Gan, C., Hu, Y., *IEEE Transactions on Industrial Electronics*, **70**(2), 1216, 2023.
[12] Augusto, A. S., Caetano, R., *Franklin Open*, **8**, 100166, 2024.
[13] Yang, S. H., Pyo, H. J., Jung, D. H., Kim, W. H., *Machines*, **11**(4), 445, 2023.
[14] Farrokh, F., Vahedi, A., Torkaman, H., Banejad, M., *IET Electrical Systems in Transportation*, **13**(2), e12074, 2023.
[15] Wu, W., Liu, X., Huang, C., Liu, Z., Liang, J., *AIP Advances*, **15**(5), 055030, 2025.
[16] Alsuwian, T., Habib, A., Zainuri, M. A. A. M., Ibrahim, A. A., Tousizadeh, M., Adam, R. H., Alhawari, A., Almawgani, A. H. M., Almasabi, S., *Alexandria Engineering Journal*, **92**, 283, 2024.
[17] Tadjuddin, M., Hasanuddin, I., Fuadi, Z., Mukminin, A., Arief, M. R., *IOP Conf. Series: Materials Science and Engineering*, **931**, 012007, 2020.
[18] Pranjić, F., Virtič, P., *Energies*, **17**(5), 1089, 2024.

[19] Tajuddin, H., Kartawidjaja, M., Wijayanti, L., Kumala Indriati, K., Tobing, S., *Jurnal Rekayasa Elektrika*, **19**(4), 135, 2023.
[20] Adem Dalcali, A., Kurt, E., Çelik, E., Öztürk, N., *Politeknik Dergisi*, **23**(1), 223, 2020.
[21] Xiao, L., Li, J., Qu, R., Lu, Y., Zhang, R., Li, D., *IEEE Transactions on Industry Applications*, **53**(2), 1018, 2016.
[22] Stan, M. F., Bancuta, I., Virjoghe, E. O., Husu, A. G., Cobianu, C., *Energies*, **17**(24), 6237, 2024.